PHYSICAL REVIEW E VOLUME 53, NUMBER 1 JANUARY 1996

Exact solutions of the monomer-monomer reaction: Segregation, poisoning, and interface evolution

David S. Sholl[1] and Rex. T. Skodje[2]
[1]*Program in Applied Mathematics, University of Colorado, Boulder, Colorado 80309-0526*
[2]*Department of Chemistry and Biochemistry, Joint Institute for Laboratory Astrophysics and Program in Applied Mathematics, University of Colorado, Boulder, Colorado 80309-0215*
(Received 16 August 1995)

The dynamics of the monomer-monomer surface reaction can be defined by an exact, closed set of differential rate equations in the limit of infinite adsorption rates. We use these equations to obtain numerically converged "exact" solutions to this model for a variety of situations that have previously been treated with Monte Carlo simulations. In particular, we derive a number of results for spatially inhomogeneous systems that involve an evolving reactive interface.

PACS number(s): 05.40.+j, 68.10.Jy, 68.35.Fx, 82.20.Mj

I. INTRODUCTION

Chemical reactions that take place on catalytic surfaces exhibit many fascinating and complex behaviors. One approach towards developing an understanding of these reactions that has attracted significant attention in recent years is to investigate highly simplified lattice gas (LG) models of surface reactions [1,2]. These models are typically investigated using Monte Carlo (MC) simulations or by using approximate mean field techniques. MC simulations are attractive since a large enough calculation is expected to converge to the true LG result. Unfortunately, many important quantities cannot be computed in practice since the MC simulations required are simply too computationally intensive. For example, extracting exponents for scaling behavior, determining finite size effects, or distinguishing between a stable and metastable configuration can easily become too difficult with MC techniques. On the other hand, a mean field treatment is much more computationally tractable since a modest set of coupled ordinary differential equations can be accurately solved using efficient numerical algorithms. The problem with the mean field approach is that the treatment is generally an approximation and quantities such as scaling exponents often are not found accurately. In this paper we consider a surface reaction model where a mean field treatment is exact: the monomer-monomer reaction [3–12]. Our main result is that it is possible to exactly calculate a number of physically relevant quantities for spatially inhomogeneous distributions of adsorbates. In particular, we consider the evolution of an initially sharp interface between regions covered by different species. This situation has been the subject of two recent MC studies [9,10]. We also show how exact solutions of the model can yield useful insights into the case when the surface is initially randomly covered by adsorbates.

The monomer-monomer model, also known as the $A + B$ reaction model, is one of the simplest examples of a model surface reaction. In this model, monomers of species A or B may adsorb onto empty surface sites,

$$A_{(g)} + E \to A_{(a)}, \tag{1}$$
$$B_{(g)} + E \to B_{(a)}, \tag{2}$$

and unlike species on adjacent sites may react and desorb,

$$A_{(a)} + B_{(a)} \xrightarrow{k} AB_{(g)} + 2E. \tag{3}$$

An unoccupied surface site is represented by E, and the subscripts (a) and (g) denote species in the adsorbed and gaseous states, respectively. A surface site may be occupied by at most one particle and the lattice is assumed to be square. We will only consider the case when the adsorption rates are infinitely faster than the surface reaction rate. In this limit, every surface site is occupied by either an A or a B monomer at all times. As we will see below, this property makes it possible to express the dynamics of the model in a closed form. However, we emphasize that, while exact solutions are only possible when this condition is met, MC simulations strongly suggest that the phenomena observed in this model are shared by more general models with finite adsorption rates [3,8]. As with other studies of this model, we also restrict our attention to the case when the adsorption rates of A and B are equal. If the adsorption rates are not equal, the surface is rapidly poisoned by the species with the faster adsorption rate [8]. All of the solutions we develop below are for two-dimensional square lattices, but our methods could also be applied to other dimensions or lattice geometries.

In Sec. II, we outline the derivation of the exact rate equations for the monomer-monomer reaction. This derivation closely follows previous work [5,6,8]. We present rate equations in two different representations. The first is useful for considering spatially averaged quantities, while the second is necessary to treat spatially inhomogeneous situations. These equations are used in Sec. III to reconsider the issue of how the reaction rate and cluster sizes of the segregated domains that form on surfaces with random initial conditions behave for large times [8,10].

1063-651X/96/53(1)/335(8)/$06.00

In Sec. IV, we consider how simulations of the monomer-monomer reaction on finite lattices may differ from infinite lattice results. As well as examining the desorptionless monomer-monomer reaction (defined above), we consider the reaction kinetics of the monomer-monomer reaction when adsorbed particles of either species are allowed to desorb with rate p. Introducing desorption into the model allows the formation of nontrivial steady states and the occurrence of more complicated reaction kinetics [5–7].

In Secs. V and VI, we derive a number of exact results for a problem that has been studied using MC simulations by Kang and Weinberg: the evolution of a reactive interface [9,10]. If the surface is initially divided into regions covered solely by one species of particles, a reactive interface forms that broadens and roughens as time progresses. In Sec. V, we derive an analytic expression for the site densities and width of this interface. We also briefly discuss another model examined by Kang and Weinberg: a lattice gas of noninteracting diffusing monomers [9]. In Sec. VI we derive the reaction rate of a broadening interface as a function of time, and discuss the roughening of such interfaces.

II. EXACT RATE EQUATIONS

The exact dynamics of any LG model with finite range interactions may be formally expressed as an infinite hierarchy of differential rate equations [13,14]. These rate equations describe the evolution of the probabilities for finding clusters of arbitrary size and composition on the lattice. In general, these hierarchies are difficult to treat, because the evolution of each type of cluster is coupled to the evolution of all other clusters. When this is the case, the rate equations can usually only be solved by introducing simplifying assumptions which break the hierarchy [14,15], although there are some examples where information can be found by direct analysis of the exact hierarchy [13,16]. One of the reasons that the monomer-monomer model has attracted the attention it has is that its hierarchy of rate equations can be exactly closed at each order [5,6,8]. In this section, we briefly review the derivation of these closed exact rate equations.

We define a set of time-dependent variables $a_{i,j}$ to be the probability that any pair of sites separated by i sites along one principal lattice direction and j sites in the other direction are simultaneously occupied by A monomers. The variable $a_{0,0}$ is the probability that a randomly chosen individual site is occupied by an A particle, and $a_{1,0}$ represents the probability that an adjacent pair of sites both contain A monomers. From the definition of $a_{i,j}$, it can be seen that $a_{i,j} = a_{\pm i,\pm j}$. Following the methods of Refs. [5], [6], and [8], it can be shown that the evolution of the pair variables $a_{i,j}$ for the monomer-monomer reaction without desorption is governed by the following set of equations which are uncoupled to higher cluster sizes:

$$\begin{aligned} &\frac{d}{dt}a_{0,0} = 0, \\ &\frac{d}{dt}a_{1,0} = k\left(a_{2,0} + 2a_{1,1} + \frac{1}{2}a_{0,0} - \frac{7}{2}a_{1,0}\right), \\ &\frac{d}{dt}a_{i,j} = k\triangle_{i,j}a_{i,j} \text{ for } |i|^2 + |j|^2 \geq 2. \end{aligned} \tag{4}$$

In the last of these equations, $\triangle_{i,j}$ is a spatially discrete Laplacian operator that is defined by

$$\triangle_{i,j}a_{i,j} = a_{i+1,j} + a_{i-1,j} + a_{i,j+1} + a_{i,j-1} - 4a_{i,j} \tag{5}$$

on a two-dimensional square lattice. These equations can easily be generalized to lattices with other geometries and dimensions [5].

It is important to note that, if $a_{i,j}$ is specified for all i and j, then all of the other site and pair densities for the system are defined. For example, the probability that an adjacent pair of sites is occupied by one A monomer and one B monomer (denoted ab) can be expressed as

$$ab = a_{0,0} - a_{1,0}. \tag{6}$$

This is an example of a lattice summation identity. All site and pair densities can be expressed as linear combinations of $a_{i,j}$'s using similar identities [8].

We emphasize that the $a_{i,j}$ are spatially averaged probabilities. It is also possible to form rate equation hierarchies in which the variables are the probabilities of finding certain clusters in specific positions on the lattice [6,8,14]. For example, we define $A_{i,j}$ to be the probability that the site at position (i,j) is occupied by an A monomer [notice that the indices (i,j) now denote the location of a specific lattice site rather than the separation between two sites as in the averaged theory]. In this case, $A_{i,j}$ is found by performing an average over an ensemble of systems with identical initial conditions. As with the averaged equations above, the evolution of $A_{i,j}$ is governed by a closed set of equations [6,8]:

$$\frac{d}{dt}A_{i,j} = \frac{k}{2}\triangle_{i,j}A_{i,j}, \tag{7}$$

where $\triangle_{i,j}$ is defined by Eq. (5). As above, if $A_{i,j}$ is known for all i and j, then all of the site densities are known. In this case, this is a consequence of the fact that $A_{i,j} + B_{i,j} = 1$. The evolution equations for the spatial pair variables can also be derived and are closed, but we will not use them below. The variables in the averaged rate equation hierarchy [Eqs. (4)] are simply the spatial averages of the variables in the hierarchy that has Eq. (7) as its lowest order equation. For example, on a finite lattice with N^2 sites,

$$a_{0,0} = \frac{1}{N^2}\sum_{i=1}^{N}\sum_{j=1}^{N}A_{i,j}. \tag{8}$$

The closed forms above for the evolution of the site and pair probabilities of the monomer-monomer reaction only exist in the special circumstance that the impingement rates of the two species are equal and infinitely faster than the surface reaction rate. If either of these conditions is not satisfied, the model can still be described by a hierarchy of rate equations, but the evolution of clusters of all sizes must be considered simultaneously if exact solutions are to be found.

Evans and Ray have noted that some other surface reaction models, notably the monomer-dimer and dimer-dimer reactions, can be described by closed, exact rate equations in the limit of infinite adsorption rates [8]. The rate equations and behaviors of these models are very similar to the monomer-monomer model. There are also a small number of other LG models that may be treated exactly, including the Glauber model [17], the randomly hopping lattice gas model [18], the equilibrium single-step model [19], and one-dimensional coagulation growth [20].

III. CLUSTER GROWTH FROM RANDOM INITIAL CONDITIONS

The most well studied initial condition for the monomer-monomer reaction is the case when the lattice is initially covered with an equal number of A and B monomers that are randomly distributed. This situation has been treated both in MC simulations [4,8,10] and by analyzing the averaged pair equations [6,8]. Qualitatively, the initially random adsorbate distribution forms segregated clusters containing only a single species which grow as time progresses. As these segregated domains grow, reactions only occur around their boundaries, so the overall reaction rate decreases monotonically with time and approaches zero as $t \to \infty$. In this section we want to briefly reconsider the question of how the reaction rate and domain sizes scale at large times.

The best way to resolve the long time behavior of this system would be to find an analytic solution to the averaged pair equations [Eqs. (4)]. Unfortunately, it has not been possible to find such a solution. A continuum limit of the pair equations that is valid on length scales much greater than one lattice spacing has been analyzed [6], but nothing can be concluded from these results about the reaction rate. A method that can yield a great deal of useful information is the numerical solution of the pair equations [8]. The initial conditions for the pair equations are $a_{0,0}(0) = 1/2$ and $a_{i,j}(0) = 1/4$ for $(i,j) \neq (0,0)$. Because of the symmetry properties of $a_{i,j}$, it is only necessary to solve the pair equations for $i \geq 0$ and $0 \leq j \leq i$. The key fact that makes the numerical solutions feasible is that at any fixed time T (on an infinite lattice) there is a distance $r_0(\epsilon, T)$ such that $|a_{i,j} - 1/4| < \epsilon$ for all $|i|^2 + |j|^2 \geq r_0^2$. By choosing a nonzero but very small ϵ, the domain of computation can be made finite. The solutions of the pair equations on this truncated domain are identical to the solutions of the pair equations of an infinite lattice for all $t < T$ [8]. The pair equations on the truncated domain are numerically integrated using standard methods for systems of ordinary differential equations. We have verified that the results below are independent of the details of the integration method.

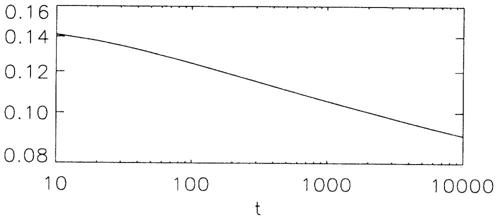

FIG. 1. The reaction rate between an adjacent pair of sites for the monomer-monomer reaction when $k = 1$. Both axes are logarithmic.

We have integrated the averaged pair equations with $k = 1$ for $t \leq 20\,000$. These computations required values of r_0 as large as 1000. The average reaction rate,

$$R = k(a_{0,0} - a_{1,0}), \tag{9}$$

is shown as a function of time in Fig. 1. As mentioned above, R decreases monotonically with time and approaches zero as $t \to \infty$. Kang and Weinberg measured $R(t)$ from MC simulations and suggested that $R \sim t^{-\omega}$ with $\omega = 0.084 \pm 0.005$ for large t [9]. Since the results from integrating the exact rate equations do not contain the fluctuations that are inherent to MC simulations, which can only be averaged over a finite number of runs, this scaling hypothesis can be directly assessed [8]. One useful way to test if $R \sim t^{-\omega}$ is to define a time-dependent exponent $\omega(t)$ by

$$\omega(t) = -\frac{t dR/dt}{R}. \tag{10}$$

If R obeys the scaling postulated above, $w(t)$ will be independent of time as $t \to \infty$. The value of $\omega(t)$ for $t \leq 20\,000$ is shown in Fig. 2. It can be seen that $\omega(t)$ decreases monotonically with time in this time range [8], and it is difficult to conclude that it approaches a nonzero value as $t \to \infty$. However, it is clear that the value of ω derived by Kang and Weinberg represents a mean value of the variable exponent. Evans and Ray suggested that the reaction rate may obey the scaling $R \sim (\ln t)^{-\sigma}$. This hypothesis may be checked by defining

$$\sigma(t) = -\frac{(t \ln t) dR/dt}{R}. \tag{11}$$

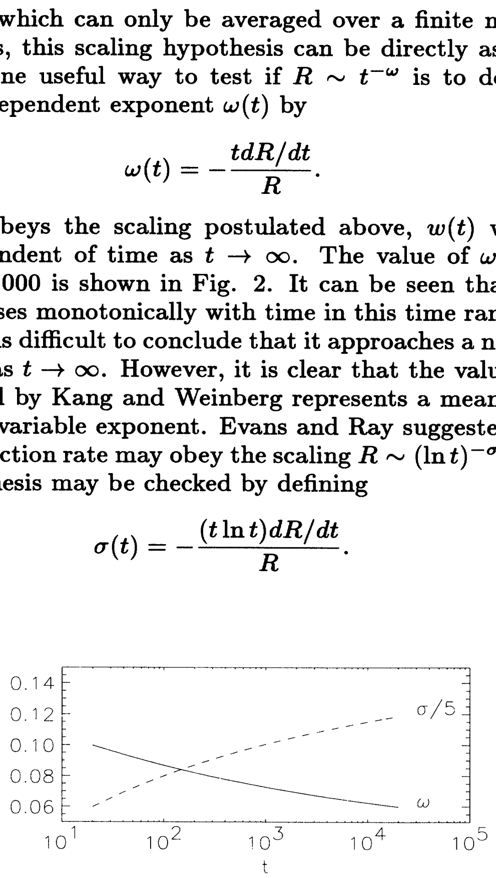

FIG. 2. The scaling exponents ω and σ as a function of time for the monomer-monomer reaction.

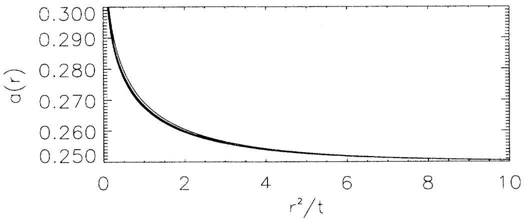

FIG. 3. The pair variables $a(r) = a_{r,0}$ plotted vs r^2/t at $t = 2500, 5000, 7500$, and $10\,000$ (top to bottom) for the desorptionless monomer-monomer reaction.

The time dependence of $\sigma(t)$ is also shown in Fig. 2. Note that it is not possible for both $\omega(t)$ and $\sigma(t)$ to be nonzero and finite as $t \to \infty$ [8]. As with $\omega(t)$, it is difficult to determine what the behavior of $\sigma(t)$ is as $t \to \infty$ from Fig. 2. At this stage, the true asymptotic scaling of $R(t)$ remains an open problem.

The growth rate of the segregated clusters can also be examined using numerical solutions of the exact pair equations. This issue has been examined by Krapivsky using an approximate continuum limit of the pair equations [6] and by Kang and Weinberg using MC methods [10]. Both of these studies concluded that the average cluster size grows as $\sqrt{t}$ for large t. As with the reaction rate, the results previously generated with MC simulations can be computed exactly using the averaged pair equations. In Fig. 3, the pair densities $a_{r,0}(t)$ are plotted versus r^2/t for several values of t. The pair densities approximately collapse onto a single curve, in agreement with the MC results of Kang and Weinberg [10]. If this collapse was exact, then the cluster size would be growing exactly as $\sqrt{t}$ for the t values shown. The results in Fig. 3 suggest that this scaling is being approached at large times.

IV. FINITE SIZE EFFECTS

Because all MC simulations must be performed on finite lattices, it is important to be able to understand how these simulations differ from LG models on infinite lattices. The monomer-monomer reaction provides a rare example in which the infinite lattice result may be directly obtained. We showed above that the averaged pair equations can directly yield information about the behavior of the monomer-monomer reaction on infinite lattices. In this section we show that similar results may be obtained for finite lattices, and the differences between these systems are discussed.

First we consider the desorptionless monomer-monomer reaction on finite lattices. It is well known that this model reaches a poisoned state in finite time, in contrast to the infinite lattice system, which exhibits a nonzero reaction rate for all finite times [5,6]. Krapivsky has shown that finite lattices become completely poisoned by either A or B on a time scale $t \sim N \ln N$, where N is the total number of lattice sites. The details of this poisoning can easily be elucidated by integrating the averaged pair equations. To represent a lattice with $(2M+1)^2$ sites and periodic boundary conditions, we use the pair equations as above with $0 \leq i \leq M$, $0 \leq j \leq i$, and $a_{M+1,j} = a_{M,j}$. This choice of indices reduces the number of equations that need to be solved by exploiting the symmetry of the equations.

The reaction rates for lattices with $M = 10$, 20, and ∞ and $k = 1$ are compared in Fig. 4. In each case, the initial condition was a random distribution of equal numbers of A and B monomers. The reaction rates are identical for small t, but at large enough t the finite lattice reaction rates plunge precipitously to zero. This occurs when the size of the segregated clusters in the system becomes comparable to the size of the lattice. This is an example of the well known principle that MC simulations on finite lattices are equivalent to infinite lattice simulations if all the length scales of correlations are much less than the size of the finite lattice [21]. These observations once again demonstrate the validity of the MC simulations of Kang and Weinberg [10].

Now we will consider the monomer-monomer reaction with desorption on finite lattices. When desorption is introduced into the model, nontrivial steady states can exist that have nonzero reaction rates [5,6]. In these steady states, the tendency of the reaction to form segregated clusters is balanced by desorption from within the clusters. Clément *et al.* derived an analytic expression describing these steady states on finite lattices [5]. This expression shows that when the desorption rate p is sufficiently large, the steady states consist of segregated clusters that are considerably smaller than the lattice [5]. This behavior also occurs on infinite lattices for any nonzero value of p. When p is sufficiently small, however, the finite lattice steady states are quite different from the infinite lattice states. In this case the segregated domains grow to cover the entire lattice, so the lattice becomes saturated [5]. The lattice cannot become completely poisoned when $p > 0$, but the reaction rate of the saturated states can be made arbitrarily small by letting p be very small. The transition between the existence of segregated and saturated equilibrium states occurs around a critical value of p, denoted p_c, which satisfies

$$p_c \ln\left(\frac{1}{p_c}\right) \simeq \frac{1}{N}, \tag{12}$$

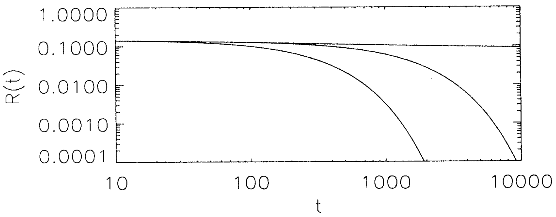

FIG. 4. The reaction rate as a function of time for the monomer-monomer reaction with random initial conditions on a 21 × 21 lattice, a 41 × 41 lattice, and an infinite lattice (lower to upper curves, respectively).

where N is the total number of sites on the lattice [7].

Flament *et al.* have shown that the kinetics of reactions that approach a segregated steady state have a different character from reactions whose final state is a saturated steady state [7]. They derived asymptotic expressions for the reaction rate at short times, and performed MC simulations to describe the general behavior. Once again, the general behavior of the system can be elucidated much more accurately by integrating the pair equations. The averaged pair equations for the monomer-monomer reaction with desorption can be expressed as

$$\begin{aligned}\frac{d}{dt}a_{0,0} &= 0,\\ \frac{d}{dt}a_{1,0} &= k\left(a_{2,0}+2a_{1,1}+\frac{1}{2}a_{0,0}-\frac{7}{2}a_{1,0}\right)\\ &\quad +p(a_{0,0}-2a_{1,0}),\\ \frac{d}{dt}a_{i,j} &= k\Delta_{i,j}a_{i,j}+p(a_{0,0}-2a_{i,j}) \text{ for } |i|^2+|j|^2\geq 2.\end{aligned} \tag{13}$$

We have calculated $R(t)$ for a 61×61 lattice with $k=1$ and with various values of p: the results are shown in Fig. 5. For this lattice, $p_c \simeq 2.5\times10^{-5}$ [using Eq. (12)]. When $p \gg p_c$ (for example, when $p=1.0\times10^{-3}$ in Fig. 5), the reaction rate decays in a simple manner to its steady state value. The steady state value can be calculated exactly [5]. This simple decay to a steady state is the qualitative behavior of the monomer-monomer reaction with desorption on an infinite lattice for any $p>0$. When $p<p_c$ (e.g., $p=1\times10^{-6}$ in Fig. 5) the kinetics are considerably more complicated. The initial decay is much like the infinite lattice result. However, as the size of the segregated clusters on the lattice becomes comparable to the total size of the lattice, the reaction rate decays more rapidly before leveling off to a steady state value. This crossover behavior was also seen in the MC simulations of Flament *et al.* [7]. The steady state reaction rate of the saturated states is considerably lower than the equilibrium rate on an infinite lattice with the same value of p [5]. Figure 5 also shows that when $p\simeq p_c$ the long term behavior of $R(t)$ is dominated by finite size effects.

The monomer-monomer reaction with desorption also exhibits a noise induced bistability when it is simulated on finite lattices [4,5,12]. This occurs because the saturated states can be dominated by either A or B particles, and over sufficiently long periods of time the system can flip between these two states. The averaged rate equation hierarchy cannot be used to study this phenomenon, because it deals only with correlations between sites at equal times [5]. We emphasize that this bistability is purely a finite size effect: it can only occur on finite lattices when p is small enough to allow saturated states to form. The existence of this type of bistability in finite systems is a well known feature of other similar LG models such as the Ising model [21].

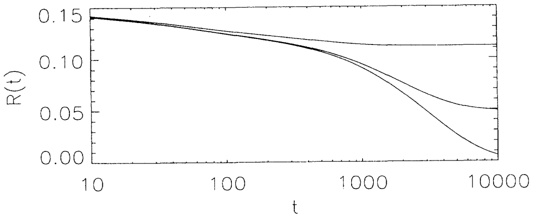

FIG. 5. The reaction rate as a function of time for the monomer-monomer reaction on a 61 × 61 lattice with $p=1\times10^{-3}, 1\times10^{-4}$, and 1×10^{-6} (upper to lower curves, respectively).

V. THE BROADENING OF REACTIVE INTERFACES

In addition to surfaces with random initial conditions, Kang and Weinberg have studied how an initially linear interface separating regions poisoned by A and B monomers evolves [9,10]. They found that the reactive interface broadens and roughens as time progresses. In particular, they found that the interface width grew as $\sqrt{t}$. In this section we derive an exact expression for the site densities and interface width that is valid for all time, which proves that this scaling is correct.

The broadening of the reactive interface is an intrinsically spatially inhomogeneous phenomenon, so it is appropriate to examine it using the spatial rate equation hierarchy [14]. As described in Sec. II, the evolution of the spatial site densities $A_{i,j}$ and $B_{i,j}$ is exactly governed by

$$\frac{d}{dt}A_{i,j}=\frac{k}{2}\Delta_{i,j}A_{i,j}, \tag{14}$$

and the conservation law $A_{i,j}+B_{i,j}=1$. The initially linear interface can be defined by the initial condition $A_{i,j}=1$ (0) for $i\leq 0$ (>0).

Krapivsky [6] showed that the general solution of Eq. (14) is

$$A_{i,j}(\tau)=e^{-2\tau}\sum_{m=-\infty}^{\infty}\sum_{n=-\infty}^{\infty}\sigma_{m,n}I_{i-m}(\tau)I_{j-n}(\tau), \tag{15}$$

where $\tau=kt$, I_n are modified Bessel functions, and the coefficients $\sigma_{m,n}$ are defined by the initial conditions as

$$\sigma_{m,n}=A_{m,n}(t=0). \tag{16}$$

For the interfacial initial conditions described above, this solution can be greatly simplified. The initial conditions are $\sigma_{m,n}=1$ (0) for $m\leq 0$ (>0). Then, since [22]

$$\sum_{n=-\infty}^{\infty}I_n(z)=e^z, \tag{17}$$

the sum over n in Eq. (15) may be evaluated explicitly, yielding

$$A_i(\tau)=e^{-\tau}\sum_{m=-\infty}^{0}I_{i-m}(\tau). \tag{18}$$

Because the site variables are independent of j, the notation in this expression has been simplified by setting $A_i = A_{i,j}$ for all j. By using Eq. (17) and the fact that $I_{-n}(z) = I_n(z)$ (when n is an integer) [22], this solution may be further simplified:

$$A_i(\tau) = \frac{1}{2}[1 + e^{-\tau} I_0(\tau)] + e^{-\tau} \sum_{n=1}^{|i|} I_n(\tau), \tag{19}$$

for $i \leq 0$. The symmetry of the initial conditions mean that $A_i(t) = 1 - A_{-i+1}(t)$ for $i > 0$. Thus the expression above exactly defines the site densities $A_{i,j}$ and $B_{i,j}$ for any i and j and for $t \geq 0$.

Kang and Weinberg measured the width of the reactive interface, ω_r, by defining $g_i = A_{i+1} - A_i$, and setting

$$w_r^2(\tau) = \frac{\sum n^2 g_n(\tau)}{\sum g_n(\tau)}, \tag{20}$$

where both of the sums over n are from $-\infty$ to ∞. Substituting the explicit solution for A_i into the definition of g_i shows that

$$g_i = -e^{-\tau} I_i(\tau). \tag{21}$$

By using Eq. (17) it can be seen that the denominator in the definition of ω_r^2 is equal to -1. The sum in the numerator can be evaluated by using the recurrence relation [22]

$$n I_n(z) = \frac{z}{2}[I_{n-1}(z) - I_{n+1}(z)]. \tag{22}$$

Substituting this into the numerator of Eq. (21) and collecting all terms that contain Bessel functions of the same order yields

$$\begin{aligned} \omega_r^2(\tau) &= 2e^{-\tau} \sum_{n=1}^{\infty} n^2 I_n(\tau) \\ &= \tau e^{-\tau} \left(I_0(\tau) + 2 \sum_{n=1}^{\infty} I_n(\tau) \right) \\ &= \tau. \end{aligned} \tag{23}$$

Thus the exact value of ω_r is $\sqrt{kt}$ for $t \geq 0$.

Kang and Weinberg also simulated the evolution of an interface for a noninteracting lattice gas of diffusing monomers [9]. In this model, the number of monomers on the lattice is fixed, and monomers hop into adjacent empty sites at rate k_h. The initial interface divides a region covered by particles ($A_{i,j} = 1$) from an empty region ($A_{i,j} = 0$). It was found that the width of the interface obeyed the same scaling as the monomer-monomer reaction, and a combinatorial argument proving this was given [9]. A more straightforward way to demonstrate this equivalence is to consider the spatial rate equations of the diffusing monomers. Deriving the exact spatial site equations as for the monomer-monomer reaction yields

$$\frac{d}{dt} A_{i,j} = k_h \triangle_{i,j} A_{i,j}. \tag{24}$$

Thus, if $2k_h = k$, *any* property of the monomer-monomer reaction site densities, for *any* initial conditions, also holds for the monomer diffusion model. The exact closure of the monomer diffusion site equations also yields a simple proof that the chemical diffusion coefficient of a noninteracting lattice gas is coverage independent [23].

The evolution equations for the pair densities of the monomer-monomer reaction and the monomer diffusion model are *not* identical. Hence any observable of these models that is a function of pair (or higher order) probabilities will have different values for the two models. One example of this property is the fact that the interface roughnesses of broadening interfaces in the two models are not equal [9].

Although the spatial site equations are spatially discrete, it is possible to derive approximate rate equations that are spatially continuous. One way to do this is to notice that if $h = 1$

$$\begin{aligned} \triangle_{i,j} A_{i,j} = \frac{1}{h^2}(&A_{i+1,j} + A_{i-1,j} + A_{i,j+1} \\ &+ A_{i,j-1} - 4A_{i,j}). \end{aligned} \tag{25}$$

If we now consider A to be a spatially continuous variable of $x = ih$ and $y = jh$ and take the formal limit $h \to 0$, we find

$$\triangle_{i,j} A_{i,j} \to \triangle A, \tag{26}$$

where $\triangle$ is the spatially continuous Laplacian operator. Thus, in this formal limit, the exact spatial site equations for the monomer-monomer reaction become the spatially continuous diffusion equation

$$\frac{\partial A}{\partial t} = \frac{k}{2} \triangle A. \tag{27}$$

We emphasize that this equation represents only an approximation to the exact equations. When the spatial rate of change of A is small over length scales of a few lattice spacings, the evolution of A in Eq. (27) and $A_{i,j}$ in Eq. (7) is very similar. On the other hand, if A varies rapidly over the same length scales, the solution of the spatially continuous equation may deviate significantly from the true (spatially discrete) solution.

VI. REACTION RATE OF BROADENING INTERFACES

We now turn our attention to calculating the time-dependent reaction rate of a broadening interface for the monomer-monomer reaction. The key to this calculation is that the reaction rate is a spatially averaged quantity, even though the underlying lattice configuration is spatially inhomogeneous. Thus the simpler averaged rate equations may be used if appropriate initial and boundary conditions are defined. To define these conditions, we consider a finite lattice with periodic boundary conditions and the initial conditions shown in Fig. 6. Because the evolution of an interface is localized around the center of the interface, the evolution of the lattice in

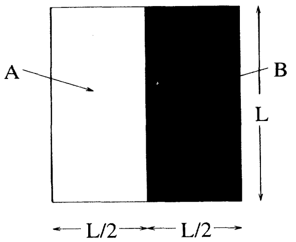

FIG. 6. The initial condition used to calculate the reaction rate of a broadening interface.

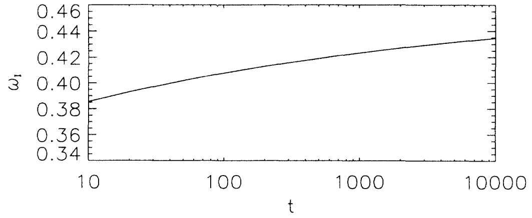

FIG. 8. The scaling exponent ω_I as a function of time for the monomer-monomer reaction with the interface initial conditions.

Fig. 6 is identical to that of an infinite lattice provided the interface width satisfies $\omega_r \ll L/2$. Thus, if the reaction rate of the finite lattice described above can be calculated, the interface reaction of an infinite lattice is known up to some finite time.

The initial conditions for the lattice pictured in Fig. 6 are $a_{i,j} = 1/2 - (i+j)/2L$ for $0 \le i \le L/2$ and $0 \le j \le L/2$. The pair variable $a_{i,j}$ is averaged over all spatial orientations of sites separated by i sites in one direction and j sites in the other direction, so $a_{i,j}$ is symmetric with respect to the interchange of i and j. The pair variables for other values of i and j are defined by symmetry conditions such as $a_{-i+L/2,j} = a_{i+L/2,j}$. The averaged pair equations [Eqs. (4)] can be integrated with the same techniques that we used in Sec. IV.

We compute the average reaction rate per row,

$$R(t) = L[a_{0,0}(t) - a_{1,0}(t)] = L\left(\frac{1}{2} - a_{1,0}(t)\right). \tag{28}$$

When $t = 0$, $R = 1/2$ for any L. The average reaction rate *per site* on the infinite lattice is trivial: it is identically zero. The time dependence of R for a lattice with $L = 2000$ and $k = 1$ is shown in Fig. 7. We have verified by computing this curve for various values of L that $R(t)$ is independent of L when $\omega_r \le L/20$. Hence the data in Fig. 7 represent the average reaction rate per row for a broadening interface on an infinite lattice with $t \le 10\,000$.

To test if $R(t)$ has a power law time dependence, $R \sim t^{\omega_I}$, we defined

$$\omega_I(t) = \frac{tdR/dt}{R} \tag{29}$$

[as in Eq. (10)]. The time dependence of $\omega_I(t)$ is shown in Fig. 8. As in Sec. II, it is possible that R asymptotically approaches a power law scaling, but it is difficult to unambiguously conclude this from our data.

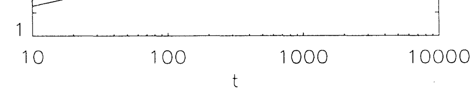

FIG. 7. The reaction rate per row for the monomer-monomer reaction with the interface initial conditions.

It is also possible to determine $R(t)$ by solving the spatial pair equations. Such solutions simultaneously yield information about how the reactions are spatially distributed. However, the computational resources necessary to solve the spatial pair equations are enormous, because each spatially distinct pair (on all length scales) must be included individually. We have performed some calculations of this type, but due to the number of equations that must be integrated they have been limited to quite short times.

One of the issues investigated by Kang and Weinberg in their MC simulations was the roughening of the reactive interface [9,10]. The roughness σ is defined as the root-mean-square position of particles that form the external perimeter. A particles in the external perimeter can be connected by nearest neighbor A (B) particles to $i = -\infty$ ($+\infty$). The external perimeter is a fractal curve with fractal dimension $d \simeq 1.33$ [9]. Kang and Weinberg showed that the data from their MC simulations suggested that the interface roughness obeyed the scaling $\sigma \sim t^{\beta}$, with $\beta = 0.455 \pm 0.005$ [9]. Unfortunately, it is not possible to calculate σ from the exact rate equations. To perform this calculation, it would be necessary to track the correlated evolution of connected clusters of all sizes up to at least the width of the interface. Although this is possible in principle because the rate equation hierarchy is closed at each order, there seems to be no practical way to realize such a calculation.

VII. SUMMARY

We have shown that the exact rate equations are a powerful tool for investigating both translationally invariant and spatially inhomogeneous states of the monomer-monomer surface reaction. These rate equations have been used to derive a variety of exact results for this reaction, including the reaction rate and cluster growth rate of surfaces with random initial conditions, finite lattice effects for the reaction both with and without desorption, and the width and reaction rate of a reactive interface. It is clear from our numerical calculations that we can greatly improve computational capabilities compared to MC simulations. We also showed how the exact, discrete equations that define the evolution of the site densities of spatially inhomogeneous states can be used to derive approximate spatially continuous equations. This procedure can also be used to derive approximate reaction-diffusion equations for more general surface reaction models [14].

We emphasize that, although the results presented here rely heavily on the exact closure of the rate equations, the general strategy of using the averaged and spatial rate equation hierarchies can be very useful in the study of more general surface reaction models. In general, the rate equations can be analyzed only after some type of approximation is made that closes the hierarchies. This approach has been used to examine, among other issues, the evolution of chemical waves and interfaces on perfect surfaces [14] and the kinetic phase diagrams of surface reactions on stepped surfaces [24].

ACKNOWLEDGMENTS

This work was supported by the National Science Foundation Grant No. CHE-9321543. We also acknowledge support from the Donors to the Petroleum Research Fund through Grant No. 27176-AC6.

[1] J. W. Evans, Langmuir **7**, 2514 (1991).
[2] V. P. Zhadanov and B. Kasemo, Surf. Sci. Rep. **20**, 111 (1994).
[3] E. Wicke, P. Kummann, W. Keil, and J. Schliefer, Ber. Bunsenges. Phys. Chem. **84**, 315 (1980).
[4] K. Fichthorn, E. Gulari, and R. Ziff, Phys. Rev. Lett. **63**, 1527 (1989).
[5] E. Clément, P. Leroux-Hugon, and L. M. Sander, Phys. Rev. Lett. **67**, 1661 (1991).
[6] P. L. Krapivsky, Phys. Rev. A **45**, 1067 (1992).
[7] C. Flament, E. Clément, P. Leroux-Hugon, and L. M. Sander, J. Phys. A **25**, L1317 (1992).
[8] J. W. Evans and T. R. Ray, Phys. Rev. E **47**, 1018 (1993).
[9] H. C. Kang and W. H. Weinberg, Phys. Rev. E **48**, 3464 (1993).
[10] H. C. Kang and W. H. Weinberg, J. Chem. Phys. **100**, 1630 (1994).
[11] E. Clément, P. Leroux-Hugon, and P. Argyrakis, Phys. Rev. E **49**, 4857 (1994).
[12] F. Moiny *et al.*, Surf. Sci. **325**, L392 (1995).
[13] J. W. Evans, Rev. Mod. Phys. **65**, 1281 (1993).
[14] D. S. Sholl and R. T. Skodje, Surf. Sci. **334**, 305 (1995).
[15] R. Dickman, Phys. Rev. A **34**, 4246 (1986).
[16] J. W. Evans and M. S. Miesch, Surf. Sci. **245**, 401 (1991).
[17] R. J. Glauber, J. Math. Phys. **4**, 294 (1963).
[18] J. W. Evans and D. K. Hoffman, Phys. Rev. B **30**, 2704 (1984).
[19] M. Plischke, Z. Racz, and D. Liu, Phys. Rev. B **35**, 3485 (1987).
[20] C. R. Doering, M. A. Burscka, and W. Horsthemke, J. Stat. Phys. **65**, 953 (1981).
[21] K. Binder and D. W. Heermann, *Monte Carlo Simulations in Statistical Physics* (Springer-Verlag, Berlin, 1992).
[22] *Handbook of Mathematical Functions*, edited by Milton Abramowitz and Irene A. Stegun (Dover, New York, 1970).
[23] R. Kutner, Phys. Lett. **81A**, 239 (1981).
[24] D. S. Sholl and R. T. Skodje, Surf. Sci. (to be published).